Viscoelastic Properties of Isolated Collagen Fibrils

Zhilei Liu Shen,[†] Harold Kahn,[‡] Roberto Ballarini,[§*] and Steven J. Eppell[†*]
[†]Department of Biomedical Engineering and [‡]Department of Materials Science and Engineering, Case Western Reserve University, Cleveland, Ohio; and [§]Department of Civil Engineering, University of Minnesota, Minneapolis, Minnesota

ABSTRACT Understanding the viscoelastic behavior of collagenous tissues with complex hierarchical structures requires knowledge of the properties at each structural level. Whole tissues have been studied extensively, but less is known about the mechanical behavior at the submicron, fibrillar level. Using a microelectromechanical systems platform, in vitro coupled creep and stress relaxation tests were performed on collagen fibrils isolated from the sea cucumber dermis. Stress-strain-time data indicate that isolated fibrils exhibit viscoelastic behavior that could be fitted using the Maxwell-Weichert model. The fibrils showed an elastic modulus of 123 ± 46 MPa. The time-dependent behavior was well fit using the two-time-constant Maxwell-Weichert model with a fast time response of 7 ± 2 s and a slow time response of 102 ± 5 s. The fibrillar relaxation time was smaller than literature values for tissue-level relaxation time, suggesting that tissue relaxation is dominated by noncollagenous components (e.g., proteoglycans). Each specimen was tested three times, and the only statistically significant difference found was that the elastic modulus is larger in the first test than in the subsequent two tests, indicating that viscous properties of collagen fibrils are not sensitive to the history of previous tests.

INTRODUCTION

Type I collagen is the most abundant animal protein. It is found in tendon, ligament, skin, bone, cartilage, heart valve, cornea, and other tissues (1). Collagenous tissues usually have well organized hierarchical structures. For example, tendon has five distinct substructures, including the collagen molecule, the collagen fibril, the fibril bundle, the fascicle, and the whole tendon (2). Collagenous tissues also contain water and ground substance (mainly proteoglycans). Improved understanding and prediction of the mechanical behavior of collagenous tissues requires knowledge of the mechanical properties at different lengthscales, the interactions between the substructures, the effect of each substructure on the overall mechanical properties, and the contributions of different phases (collagen, ground substance, and water) to the observed mechanical behavior. Though it is well known that collagenous tissues are viscoelastic (3), the origins of this viscoelasticity and mechanisms for how forces are transferred from the lower hierarchical levels to higher ones are not fully understood.

Extensive studies on viscoelastic behavior at the tissue level were reported over the last few decades. Creep tests were performed on tendons (4–7), heart valves (8), and skin (9). Stress relaxation tests were carried out on tendons (7,10–18), ligaments (17,19–22), heart valves (8,23,24), skin (9), bone (25), and cartilage (26,27). Phenomenological models including constitutive models consisting of springs and dashpots (28), and models consisting of simple exponential decay functions (7,23,25) have been used to model these experimental results. The most popular model used to explain the viscoelastic behavior of collagenous tissues is the quasilinear viscoelastic (QLV) model developed by Fung (29,30) and improved by others (11,19,31,32). It successfully described the viscoelastic behavior of tendon (10,13,33,34), ligament (20,22,33–35), and heart valve (8). Fung's model utilizes five parameters to explain the complex viscoelastic behavior of collagenous tissues and allows easy, direct comparisons among the studies carried out by different research groups and performed on different species and tissue types.

At the fibrillar level, direct mechanical measurements have only recently become possible. Atomic force microscopy (AFM)-based nanoindentation (36–39), tensile (40,41), and bending (42–44) tests, and microelectromechanical systems (MEMS)-based tensile tests (45–47) have been used to explore the quasistatic mechanical properties of single collagen fibrils. AFM-based studies have the benefit of using instrumentation widely available to many investigators. Nanoindentation was successfully used to investigate elastic modulus and hardness of single fibrils. Because of tip curvature, the actual loading of the fibril by the AFM probe tip is complex. It is expected that the majority of the applied force is along the fibril radial direction, with some force vectors also pointing along the axial direction. In general, we consider this technique to be complementary to the MEMS technique, with indentation providing primarily radial direction mechanics and MEMS providing primarily axial direction mechanics. Axial mechanical properties of single fibrils have been studied using tensile and three-point bending experiments, but these methods were limited to strains of only a few percent. They did not provide any strength or work of fracture data. A MEMS-based technique developed by our group was used to perform large-strain

Submitted October 7, 2010, and accepted for publication April 25, 2011.

*Correspondence: sje@case.edu or broberto@umn.edu

Zhilei Liu Shen's present address is Department of Biomedical Engineering, Lerner Research Institute, Cleveland Clinic, Cleveland, OH.

Editor: Charles W. Wolgemuth.

0006-3495/11/06/3008/8 $2.00

doi: 10.1016/j.bpj.2011.04.052

uniaxial tensile tests on collagen fibrils in air at ambient humidity (45,46) and in vitro with specimens completely immersed in 1× PBS buffer (47). While our previous studies measured mechanical properties of isolated collagen fibrils such as: elastic modulus, yield strength/strain, fracture strength/strain, and work of fracture via the quasi-static tensile tests, we were unable to measure viscoelastic properties. To our knowledge, there is only one published study that provides direct evidence of viscoelastic behavior at the single-fibril level. That study was an AFM-based tensile testing study, and it demonstrated the strain-rate-dependent behavior of single collagen fibrils isolated from human patellar tendon (48). However, it was a short case study based on only two specimens, and it did not provide viscoelastic properties such as relaxation time.

The objective of this work was to use quantitative experimental data of the time-dependent response of isolated collagen fibrils to determine fibril-level viscoelastic properties. In vitro coupled creep and stress relaxation tests were performed on eight type I collagen-fibril specimens using a MEMS-based technique (49). By fitting the stress-strain-time data to a constitutive model consisting of three springs and two dashpots (the Maxwell-Weichert model), we determined the elastic moduli and relaxation times of isolated collagen fibrils. To our knowledge, this is the first time relaxation times for isolated collagen fibrils have been measured.

MATERIALS AND METHODS

MEMS devices

MEMS devices (Fig. 1 *a*) designed and fabricated to perform in vitro coupled creep and stress relaxation tests on collagen fibrils were similar to those used in our previous in vitro fracture study (47). The MEMS devices were calibrated using standard finite element analysis methods (50). The main difference is that the force gauge beam of the current MEMS device is longer than that used in our previous in vitro fracture study (47), 300 μm instead of 100 μm. When we designed the MEMS devices for our previous in vitro fracture experiments (47), we tried to match the stiffness of the force-gauge beams with that of collagen fibrils measured in air. We realized later that the fibrils had significantly lower modulus in vitro than in air which meant that the force-gauge beams were stiffer than desired. To improve the force sensitivity, we chose longer, more compliant force gauge beams for the MEMS devices used in the current study. The minimum force that the current MEMS device can measure is ~0.05 μN, which is ~1/18 of the minimum force of the device used in our previous in vitro fracture test (~0.89 μN).

To obtain stress-strain curves, it was necessary to measure fibril diameter and width. Polysilicon, the material that the MEMS devices are made of, is constructed of grains a few hundred nanometers in size. This produces a cobblestonelike surface that makes it difficult to distinguish the fibril specimen from the device surface using AFM or scanning electron microscopy (SEM). To achieve a smooth substrate, we coated the fixed pads of the MEMS devices with polyimide.

Sample preparation

Type I collagen fibrils were isolated from the dermis of sea cucumber, *Cucumaria frondosa* (51). This structure has a length of several dozen microns and a diameter of 10–500 nm and is obtainable as an isolated fibril. Dark-field illumination was used to visualize fibrils in solution, because they showed very little contrast under bright field illumination. The method used to manipulate the fibrils out of solution and to fix them onto MEMS devices was the same as previously described (47).

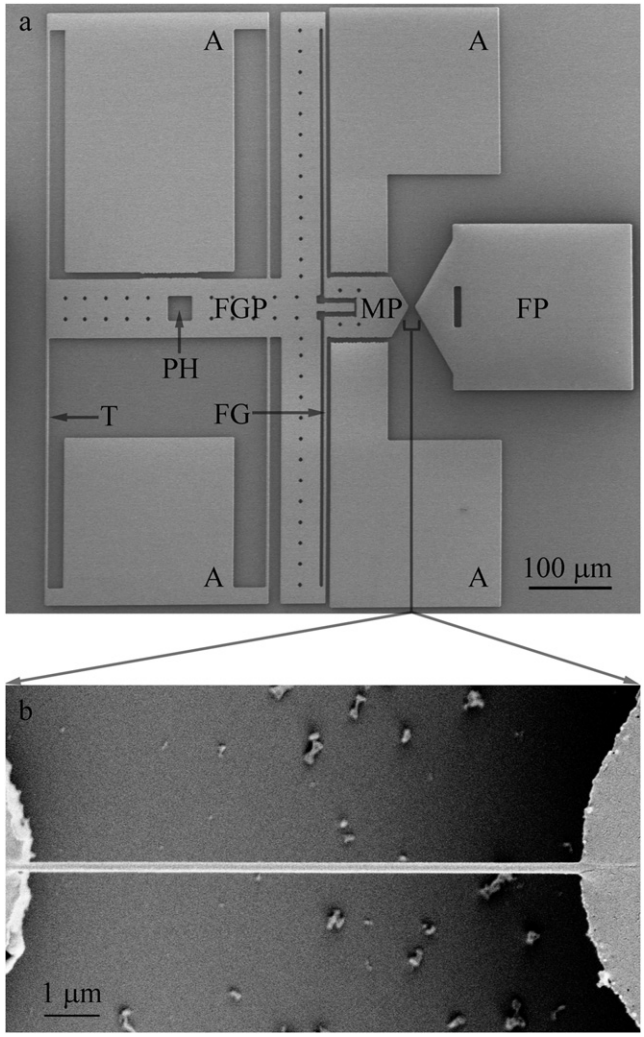

FIGURE 1 Representative MEMS device for performing a coupled creep and stress-relaxation test on collagen fibril specimens in vitro. (*a*) A low-magnification SEM image of the MEMS device, consisting of a fixed pad (*FP*), a movable pad (*MP*), a force-gauge pad (*FGP*), four anchor pads (*A*), four tether beams (*T*), a pushing hole (*PH*), and a force gauge (*FG*) consisting of two tether beams connecting the force-gauge pad and the movable pad. Compared with the MEMS devices used in our previous in vitro fracture study (47), force-gauge sensitivity was improved by using longer, more compliant tether beams. (*b*) A higher-magnification SEM image of a collagen-fibril specimen attached to movable and fixed pads of a MEMS device. Note that testing was done under in vitro conditions before taking such SEM images.

In vitro coupled creep and stress relaxation testing protocol

MEMS devices with fibril specimens attached were mounted on a single-axis-of-motion piezo stage (Nano-H100, Mad City Labs, Madison, WI). A sharp tungsten probe (with a tip diameter of ~10 μm) attached to a mechanical micromanipulator (Series 461, Newport, Irvine, CA) was

placed in the pushing hole (Fig. 1 *a*, *PH*) holding the movable portion of the device stationary. A function generator (DS345, Stanford Research Systems, Sunnyvale, CA) was used to generate a ramp-up, hold, and ramp-down function. The voltage output of the function generator was input to a controller (Nano-Drive, Mad City Labs) used to drive the piezo stage. The fixed portion of the device was moved together with the piezo stage from a displacement of 0 to ~6 μm in 1 s, held at the maximum displacement for 300 s, and then returned to zero displacement in 1 s. This protocol was repeated twice for a total of three tests per specimen with a resting time of 100 min between tests. A 60× water immersion objective lens (Fluor 60×, Nikon, Tokyo, Japan) was used to visualize the devices in PBS buffer using dark-field illumination. A digital camera (Micropublisher 3.3 RTV, QImaging, Surrey, British Columbia, Canada) was used to capture images at a frame rate of ~2 frames/s while the specimens were being stretched in-vitro at room temperature (20–25°C). The relative displacement between fixed and movable pads was controlled by the piezo stage and the sharp probe. The total displacement of the MEMS device was equal to the sum of the fibril-specimen displacement and the force-gauge displacement (i.e., $d_{total} = d_{fibril\ \ specimen} + d_{force\ \ gauge}$). There was no way to independently control the displacement of the fibril specimen and the displacement of the force gauge (i.e., the applied force). Thus we did not have a pure displacement-control or force-control testing system. A pure creep test requires a constant stress applied on the specimen, whereas a pure stress relaxation test requires a constant strain applied on the specimen. Since we did not control the displacement and the force separately, the test performed in this study is a coupled creep and stress relaxation test instead of a pure creep or a pure stress relaxation test. Care was taken to ensure that the specimens did not dry by adding PBS droplets to the specimens every 30 min. During some of the tests, insufficient stability of the experimental set-up caused drift in the displacement before the strain was relieved after 300 s. In these cases, the data after drift began were discarded. In all cases shown below, at least 60 s of drift-free behavior was observed.

Stress-strain-time relationship

Elongation of the fibril specimen and deformation of the force gauge were obtained via digital image correlation as described previously (47). Deformation of the force gauge was converted to force applied to the specimen using the force-displacement response of the force-gauge beams obtained via finite-element analysis. SEM (Hitachi S4500, Japan) was used to record radial and axial lengths needed to obtain the cross-sectional area (A_0) and the initial gauge length (l_0), respectively. All specimens were sputter-coated with ~5 nm of palladium before SEM observation. Fig. 1 *b* shows a fibril specimen spanned across the movable and fixed pads of a MEMS device. Since the sputter-coating and SEM imaging were done after the mechanical testing was finished, these procedures did not influence the measured viscoelastic properties of the fibrils. However, we expected fibrils to dehydrate in the SEM vacuum chamber resulting in aberrantly small radial measurements. We showed in a previous study that the fibril diameter in vitro is ~2.20 times larger than that in vacuo using SEM and AFM (47). In this work, we corrected the SEM-measured in vacuo fibril diameter by multiplying by this factor of 2.20. The nominal stress (σ) is obtained by dividing the applied force (F) by the initial cross-sectional area (A_0), $\sigma = F/A_o$. The engineering strain (ε) is obtained by dividing the measured change in length (d) by the initial gauge length (l_0), $\varepsilon = d/l_0$. The time of collection for each image was obtained by multiplying the image number with the time interval between two adjacent images. Thus, nominal stress versus time and engineering strain versus time curves were obtained.

A constitutive model: the Maxwell-Weichert model

Viscoelastic properties, in particular elastic modulus and relaxation times, were obtained by fitting the stress-strain-time data with the Maxwell-Weichert phenomenological model. The simplest version of the model consists of two Maxwell elements (a spring in series with a dashpot) in parallel with an additional spring, as shown in Fig. 2. The motivation for its use is that it is associated with two distinct relaxation times; models with a single relaxation time were found to be insufficient to accurately fit the experimental measurements. The relaxation modulus as a function of time for the Maxwell-Weichert model can be expressed as

$$E_{relax}(t) = E_0 + E_1 \exp\left(-t/\tau_1\right) + E_2 \exp\left(-t/\tau_2\right), \quad (1)$$

where E_0 is the time-independent elastic modulus, and the relaxation time τ_i of each Maxwell element is equal to the coefficient of viscosity of the dashpot, η_i, divided by the elastic modulus of the spring, E_i. Our experiment is neither a pure creep (constant stress) nor a pure stress relaxation (constant strain) test, but the relaxation modulus can be determined at all times, since both stress and strain are measured experimentally. The three elastic moduli (E_0, E_1, and E_2) and the two relaxation times (τ_1 and τ_2) were used as fitting parameters to perform a least-squares fit of the data.

Equation 1 was derived assuming the strain rate after application of the load was zero, which is not strictly true in these tests, although the average strain rates of $\approx 0.0002\ s^{-1}$ are very low. More specifically, the derivation assumes that the strain rate times the elastic modulus of the Maxwell elements is small compared to the stress change rate ($d\sigma_i/dt >> E_i d\varepsilon_i/dt$). For the fibril tests presented here, at short times, the stress change rate of the faster responding Maxwell element is >10 times greater than the strain rate times the elastic modulus ($d\sigma_1/dt > 10 \times E_1 d\varepsilon/dt$), and at long times, the same is true of the slower-responding Maxwell element ($d\sigma_2/dt > 10 \times E_2 d\varepsilon/dt$). Therefore, we consider Eq. 1 to be a reasonable approximation of the fibril behavior measured in this study.

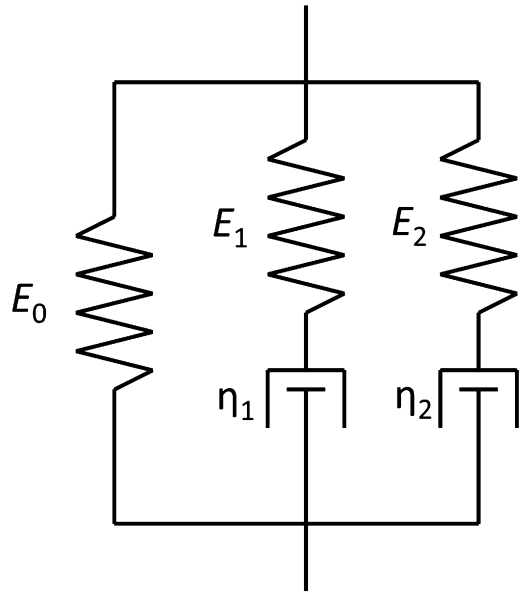

FIGURE 2 Schematic representation of the Maxwell-Weichert model used to interpret the mechanical response of the collagen fibrils. Two Maxwell elements with moduli E_1 and E_2 and viscosities η_1 and η_2 provide a model with two relaxation times τ_1 and τ_2, respectively. Equation 1 in the Materials and Methods section shows how the various constitutive parameters are used to obtain a relaxation modulus, which is then used to fit experimental curves, as shown in Fig. 4.

RESULTS

Stress-strain-time relationship of collagen fibril specimens

In vitro coupled creep and stress relaxation tests were performed on eight collagen fibril specimens. The in vacuo measured specimen diameters ranged from 100 nm to 260 nm. To account for swelling due to hydration, the in vacuo diameter was enlarged 2.20 times to obtain the in vitro diameter range of 220–570 nm, similar to that obtained in our previous in vitro fracture tests (210–450 nm) (47). The gauge lengths ranged from 9.5 to 10.6 μm. Each specimen was stretched to an initial strain between 14% and 30% (mean $\pm$ SD = 21% $\pm$ 4%). This range in the initial strains existed for two reasons. First, each specimen had a different gauge length determined by the spacing between the epoxy droplets holding the test specimen down. Second, the deformation of each specimen was different due to the fact that we did not have a displacement-control experimental set-up.

Fig. 3 displays the mechanical response of a representative collagen fibril specimen during a coupled creep and stress relaxation test. Error bars indicate the measurement uncertainties. In Fig. 3 *a*, it can be seen that the nominal stress initially had a rapid relaxation rate, which reduced in time such that the overall relaxation tended toward an asymptotic equilibrium level, which was similar to typical stress relaxation behavior. Fig. 3 *b* shows that the engineering strain of the fibril specimen increased rapidly at the beginning of the test and gradually reached a plateau similar to typical creep behavior, consisting of a primary creep (which starts with a rapid strain rate and slows with time) and a secondary creep (which has a relatively uniform strain rate). Both the stress versus time and strain versus time curves indicated that the collagen fibril specimen was viscoelastic.

Viscoelastic properties obtained from the data using the Maxwell-Weichert Model

Fig. 4 shows the relaxation modulus versus time curves of a fibril specimen that was tested three times. The fitted curves agreed well with the experimentally measured data, with $R^2 > 0.96$. However, the common tertiary creep (accelerating strain rate) and creep rupture were not observed. The reason is probably that we did not have a pure creep test at a constant stress, meaning the stress decreased as the strain increased. Therefore, the specimens had chances to relax and they never experienced the tertiary creep and creep rupture. It is clear that any damage accumulated during creep (with an initial strain up to 30%) was not enough to rupture the fibril specimens. The relaxation modulus-time curve (Fig. 4) shows that the relaxation behavior was greatest during the first few seconds, reaching >50% of the change recorded at 100 s within the first 10 s.

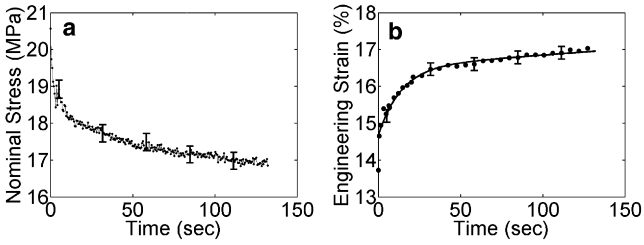

FIGURE 3 Mechanical response of a representative collagen fibril specimen. (*a*) Nominal-stress-time curve, $\sigma(t)$. (*b*) Engineering-strain-time curve, $\varepsilon(t)$. For the sake of clarity, the error bars are shown every 50 data points for both curves, and the symbols are shown every 3, 5, or 10 data points for the engineering-strain-time curve. The line represents the fitted curve, $\varepsilon(t) = -1.86e^{-0.07t} + 0.003t + 16.5$.

Comparison of viscoelastic properties of collagen-fibril specimens obtained in three tests

Table 1 lists the viscoelastic parameters enumerated in Eq. 1. Fig. 5 shows whether or not these parameters changed with each subsequent test. The elastic modulus and viscous parameters are plotted in Fig. 5, *a* and *b*, respectively. The percentage differences of any two of the three tests, X&Y, is equal to testY $-$ testX/testX $\times$ 100%, where X&Y could be test 1&2, test 1&3, or test 2&3. The error bars indicate one standard deviation. A paired Student's *t*-test was used to compare the mechanical properties obtained on these eight fibril specimens in three rounds of tests. Fig. 5 *a* shows that the time-independent elastic moduli (E_0) obtained in test 2 and test 3 were significantly lower than those obtained in test 1 ($p < 0.001$). The fast relaxation component of the modulus (E_1) was also significantly lower in the third test than in the first test ($p < 0.001$). There was no significant difference in either the time-independent or the time-dependent moduli between tests 2 and 3. Furthermore, there was no statistically significant difference in the slow relaxation component of the modulus (E_2) (Fig. 5 *a*) or the relaxation times (τ_1 and τ_2) among the three tests (Fig. 5 *b*).

DISCUSSION

Viscoelastic properties obtained from the data using the Maxwell-Weichert model

In summary, the stress versus time, strain versus time, and relaxation modulus versus time curves obtained in this study all suggest that isolated collagen-fibril specimens are intrinsically viscoelastic. This finding agrees well with an AFM-based study (48) that demonstrated the strain-rate-dependent viscoelastic behavior of single human patellar tendon fibrils.

Elastic modulus

The time-independent elastic modulus, E_0, of the fibril specimens measured on the first pull was 140 $\pm$ 50 MPa (80–250 MPa). This fell within the range measured in our

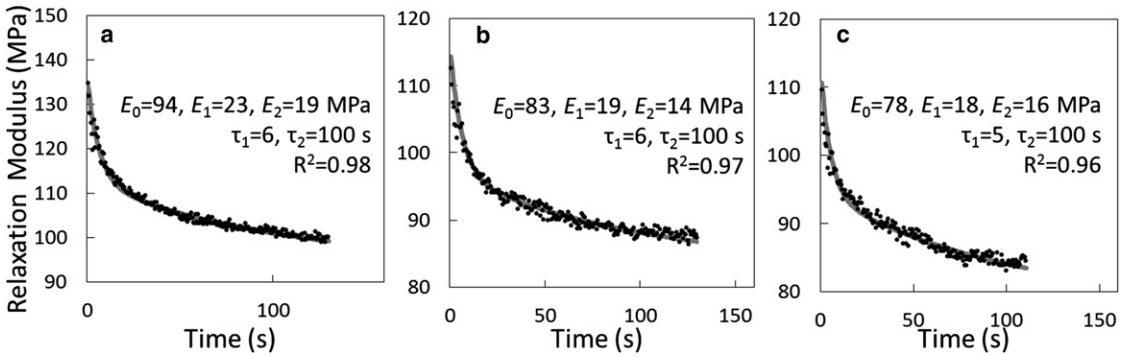

FIGURE 4 Viscoelastic behavior of the collagen-fibril specimen shown in Fig. 3 tested three times with 100 min rest between tests, showing the relaxation-modulus-time curves for (*a*) test 1, (*b*) test 2, and (*c*) test 3. Dots represent the experimental data, and solid curves represent the fitted curves using a Maxwell-Weichert model. Elastic moduli (E), relaxation times (τ), and goodness-of-fit (R^2) are shown within each subplot.

previous in vitro monotonic strain-to-fracture tests (110–1470 MPa) (47), although it was toward the lower end. In our previous study, in which we slowly strained each fibril to failure, we saw strain-dependent modulus-reducing behavior. Our results here and in the previous study are consistent with the notion that our initial strain of ~20% in the time-dependent tests took us into this reduced-modulus region. Thus, our reported value here is likely some combination of the high initial slope and the lower subsequent slopes measured previously.

The value of 140 MPa we report here also agrees within a factor of 3 with a recent multiscale model of collagen-fibril mechanics (52). However, in that model, the stress-strain curve shows nonlinear strain-hardening. Our 20% strain should have placed us in the high-strain region of the modeled curve showing a modulus closer to 2 GPa rather than the low-strain-modeled modulus of ~300 MPa. It is possible that the multiscale model does not include all of the time-dependent behavior of the collagen fibril. The model showed equilibration after 20 ns, whereas we found time-dependent behavior in the 1–100 s range.

The fitted value for E_0 fell by ~15% after the first test but did not significantly fall after this. This indicates that damage that occurred upon the first pull lowered the stiffness of the fibril, similar to the result we reported previously using similar MEMS devices to cyclically load collagen fibrils (46).

Relaxation time

Fits to our data clearly showed that more than one time constant was needed to model the data. The simplest model that gave good fits had two time constants with a fast time response around 10 s and a slow time response around 100 s.

The spread in the viscoelastic properties obtained in the coupled creep and stress relaxation test is relatively large. This variability can be attributed to two factors. First, a limited number of specimens were tested due to the difficulty in performing these experiments. Second, interspecimen variability may be present due to different cross-link densities, fibril geometries, and packing configurations of molecules within the fibrils.

Comparison of viscoelastic properties of collagen-fibril specimens obtained in three tests

The three sequential tests we performed on each fibril allowed us to determine the effect of stress-strain history on the viscoelastic properties of collagen fibril specimens. As shown in Fig. 5 *a*, the elastic modulus is always higher in the first test than in subsequent tests. This agrees well with our previous in-air tensile tests (46), indicating that something unique happens during the first load that affects the elastic modulus. The other two findings, including 1), no significant difference in the elastic modulus between test 2 and test 3, and 2), no significant difference in the relaxation time among three tests, indicate that these mechanical parameters are not changed irreversibly as a consequence of the first load/unload cycle. This is important for future experiments that aim to test the effects of further treatments such as cross-linking and/or mineralization on fibril

TABLE 1 Best-fit viscoelastic parameters using the Maxwell-Weichert model

	E_0 (MPa)	E_1 (MPa)	E_2 (MPa)	τ_1 (s)	τ_2 (s)	R^2
Test 1 (N = 8)	140 ± 50 (80–250)	18 ± 4 (11–23)	20 ± 9 (8–35)	8.1 ± 2.0 (6–12)	100 ± 5 (100–110)	0.95 ± 0.03 (0.90–0.98)
Test 2 (N = 8)	120 ± 40 (70–210)	11 ± 6 (6–22)	13 ± 4 (7–17)	7.1 ± 3.2 (4–13)	100 ± 0 (100–100)	0.91 ± 0.05 (0.82–0.96)
Test 3 (N = 8)	110 ± 40 (60–190)	10 ± 4 (6–18)	13 ± 3 (8–18)	6.6 ± 1.3 (5–9)	100 ± 6 (90–110)	0.92 ± 0.05 (0.83–0.96)
Mean of all tests	123 ± 46	13 ± 6	16 ± 7	7 ± 2	102 ± 5	0.93 ± 0.04

Summary of the constitutive parameters, as defined in Eq. 1, including the time-independent elastic modulus, E_0, characteristic modulus-and-relaxation-time pairs for a fast-response element, E_1, τ_1, and a slow-response element, E_2, τ_2, and the goodness-of-fit parameter for the fitted curves, R^2. Each value is listed as a mean ± SD with the total range of values in parentheses.

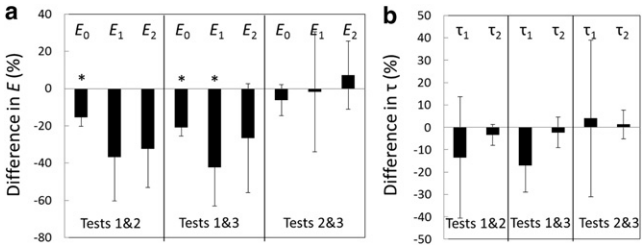

FIGURE 5 Comparison of viscoelastic properties of collagen-fibril specimens obtained in three tests, including the elastic modulus (*a*), and the relaxation time (*b*). The percentage difference of tests X&Y is equal to testY − testX/testX × 100%, where X&Y could be 1&2, 1&3, or 2&3. The standard derivation is indicated by the error bar. A paired Student's *t*-test showed that the elastic moduli obtained in tests 2 and 3 were significantly lower (*$p < 0.001$) than those obtained in test 1, whereas no significant difference was found between the elastic moduli obtained in tests 2 and 3. Furthermore, there was no statistically significant difference in the relaxation time among the three tests.

mechanics. Since this study and our previous studies (46,47) all show that there is a wide spread in the mechanical properties of single collagen fibrils, it is best to test the effects of further treatments on the same specimens to avoid interspecimen variability.

Possible mechanisms of the viscoelastic behavior of isolated collagen-fibril specimens

Viscoelasticity of soft tissues has been attributed to "the friction created by the relationships that exist between collagen fiber and the other matrix components, as well as the friction resulting from the movement of water between these components" (16). What is the cause of the viscoelastic behavior of a single collagen fibril? We propose that molecular rearrangement of collagen molecules and water molecules provide the mechanism for viscoelastic behavior of single collagen fibrils. When a stress is applied to a fibril, the collagen and water molecules inside the fibril could rearrange in a few different ways. First, the collagen molecules themselves may unwind and straighten. Second, the collagen molecules may slide with respect to one another. Third, the water molecules surrounding the collagen molecules may rotate, translate within the fibril, or be expelled from the fibril, resulting in rearrangement of the water network. Thus, these water rearrangements may occur anywhere from the 0.5-nm lengthscale (radial collagen molecule spacing within the fibril) up to the 100-nm lengthscale (fibril diameter). It may be possible to use Raman spectroscopy to measure energetic changes related to these water rearrangements (53,54). These rearrangements could create a back stress in the fibril. When the magnitude of this back stress equals that of the applied stress, the fibril no longer creeps. When the applied stress is taken away, the accumulated back stress causes the collagen molecules and water molecules within the fibril to rearrange. This process is repeatable as our results show that the relaxation-modulus-time curves obtained in the second and third tests were similar to that of the first test.

Comparison with other collagenous structures (i.e., tissues and collagen molecules)

At the tissue level, Fung's QLV model (29,30) is widely used to describe the viscoelastic response of many collagenous tissues. In the QLV model, stress is defined as the convolution of the time-dependent reduced relaxation function, $G(t)$, with the time derivative of the instantaneous elastic stress function, σ^e. Using the QLV model, sheep flexor tendons were shown to have a short relaxation time of ~2 s and a long relaxation time of ~1500 s (11). In a similar way, goat femur-medial-collateral-ligament-tibia complexes were shown to have a short relaxation time of ~2 s and a long relaxation time of ~2200 s (19).

At the fibrillar level, we showed that the viscoelastic response is well described using a five-element linear viscoelastic constitutive model, the Maxwell-Weichert model. Compared to the long relaxation time of soft tissues (1500–2200 s) obtained using Fung's QLV model, the long relaxation time of a single fibril (~100 s) is an order of magnitude smaller. The short relaxation time of the single isolated fibril is, conversely, three to four times longer than the bulk tissue. This is hard to explain based on first principles and may be more an artifact of the phenomenological fitting. Another possibility is that the differences in time behavior arise from differences in tissue source. We have further tests planned using mammalian tendon tissue that will remove the uncertainty related to fibril source. Given the data in hand at this point and assuming that model type and tissue source are not sufficient to explain an order-of-magnitude difference in relaxation time, our results suggest that the relaxation time of whole tissues is determined by components other than the collagen fibrils, most likely the ground substance (i.e., proteoglycans). This finding agrees well with a previous stress relaxation study on the mitral valve anterior leaflet (23). Using a single exponential model, it showed that the time constant for the reduction in collagen fibril strain was 8.3 min, which was smaller than the tissue-level stress relaxation time constants of 22.0 and 16.9 min in the circumferential and radial directions, respectively. The collagen fibril strain was determined by small angle x-ray scattering and was an average response of thousands of fibrils rather than the response of single fibrils. Also, the fact that the fibrils were embedded in a proteoglycan matrix may have prevented them from relaxing according to their native viscosity. This may explain the longer (8.3-min) relaxation time of the whole tissue compared with our isolated fibrils (100 s). In a more general sense, the trend that the fibrillar relaxation time is smaller than the tissue-level relaxation time agrees with our results.

At the molecular level, molecular dynamic simulation studies showed that the relaxation time of a single collagen molecule is on the order of nanoseconds (55,56). Recall that the relaxation time of a single collagen fibril is on the order of 10 s, as shown in this study, and the relaxation time of collagenous tissues is on the order of 1000 s. There seems to be a trend that the larger the hierarchical level of the collagenous structure, the longer the relaxation time becomes.

SUMMARY

We performed in vitro coupled creep and stress relaxation tests on type I collagen-fibril specimens using MEMS devices. The results suggest that isolated collagen fibrils are intrinsically viscoelastic. Using a simple Maxwell-Weichert model to fit the experimental data, we found a time-independent elastic modulus of 140 $\pm$ 50 MPa upon initial loading to ~20% strain. Subsequent loads showed a drop to ~115 $\pm$ 41 MPa. Time-dependent behavior was well fit using a two-time-constant model with a fast relaxation time of 7 $\pm$ 2 s and a long relaxation time of 102 $\pm$ 5 s. To our knowledge, this is the first time that the relaxation times of isolated collagen fibrils have been measured. The long relaxation time of isolated fibrils is an order of magnitude shorter than the long relaxation time of tendons and ligaments determined by Fung's QLV model. This is consistent with collagen fibrils contributing a fast viscoelastic behavior to collagenous tissues, with other tissue components providing the longer-duration viscous behavior. Paired Student's *t*-tests show that the collagen-fibril specimens displayed statistically higher elastic moduli during the first load compared to subsequent loads. No significant difference was found between the second and third load cycles. Furthermore, there was no statistically significant difference in the relaxation time among the three tests. This suggests that loading/unloading the fibrils twice is enough to achieve repeatable mechanical response, and may serve as a preconditioning procedure in future studies whose aim is to investigate the effects of treatments such as cross-linking and mineralization.

We thank Prof. John A. Trotter of the University of New Mexico for providing the isolated collagen fibrils, Prof. Ioannis Chasiotis and Dr. Mohammad Naraghi of the University of Illinois at Urbana-Champaign for help with digital image correlation, and Prof. Markus J. Buehler of the Massachusetts Institute of Technology for enlightening conversation.

This work was funded by National Science Foundation grant 0532320, the National Institutes of Health grant 1 R21 EB004985-01A1, and the Veterans Administration through a VA Foundation Grant. The content is solely the responsibility of the authors and does not necessarily represent the official views of the National Science Foundation or the National Institutes of Health. This investigation was conducted in a facility constructed with support from Research Facilities Improvement Program grant C06 RR12463-01 from the National Center for Research Resources, National Institutes of Health. Z.L.S. was supported by an Innovation Incentive Fellowship grant from the Ohio Board of Regents. R.B. acknowledges support from the James L. Record Chair.

REFERENCES

1. Fratzl, P., editor. 2008. Collagen: Structure and Mechanics. Springer Science+Business Media, New York.
2. Silver, F. H., J. W. Freeman, and G. P. Seehra. 2003. Collagen self-assembly and the development of tendon mechanical properties. *J. Biomech.* 36:1529–1553.
3. Fung, Y. C. 1993. Biomechanics: Mechanical Properties of Living Tissues. Springer-Verlag, New York.
4. Wang, X. T., and R. F. Ker. 1995. Creep rupture of wallaby tail tendons. *J. Exp. Biol.* 198:831–845.
5. Rigby, B. J., N. Hirai, …, H. Eyring. 1959. The mechanical properties of rat tail tendon. *J. Gen. Physiol.* 43:265–283.
6. Wren, T. A., D. P. Lindsey, …, D. R. Carter. 2003. Effects of creep and cyclic loading on the mechanical properties and failure of human Achilles tendons. *Ann. Biomed. Eng.* 31:710–717.
7. Sasaki, N., N. Shukunami, …, Y. Izumi. 1999. Time-resolved x-ray diffraction from tendon collagen during creep using synchrotron radiation. *J. Biomech.* 32:285–292.
8. Grashow, J. S., M. S. Sacks, …, A. P. Yoganathan. 2006. Planar biaxial creep and stress relaxation of the mitral valve anterior leaflet. *Ann. Biomed. Eng.* 34:1509–1518.
9. Purslow, P. P., T. J. Wess, and D. W. Hukins. 1998. Collagen orientation and molecular spacing during creep and stress-relaxation in soft connective tissues. *J. Exp. Biol.* 201:135–142.
10. Johnson, G. A., D. M. Tramaglini, …, S. L. Woo. 1994. Tensile and viscoelastic properties of human patellar tendon. *J. Orthop. Res.* 12:796–803.
11. Sarver, J. J., P. S. Robinson, and D. M. Elliott. 2003. Methods for quasi-linear viscoelastic modeling of soft tissue: application to incremental stress-relaxation experiments. *J. Biomech. Eng.* 125:754–758.
12. Wu, J. J. 2006. Quantitative constitutive behaviour and viscoelastic properties of fresh flexor tendons. *Int. J. Artif. Organs.* 29:852–857.
13. Haut, R. C., and R. W. Little. 1972. A constitutive equation for collagen fibers. *J. Biomech.* 5:423–430.
14. Yamamoto, E., K. Hayashi, and N. Yamamoto. 1999. Mechanical properties of collagen fascicles from the rabbit patellar tendon. *J. Biomech. Eng.* 121:124–131.
15. Ciarletta, P., S. Micera, …, P. Dario. 2006. A novel microstructural approach in tendon viscoelastic modelling at the fibrillar level. *J. Biomech.* 39:2034–2042.
16. Screen, H. R. C. 2008. Investigating load relaxation mechanics in tendon. *J. Mech. Behav. Biomed. Mater.* 1:51–58.
17. Schatzmann, L., P. Brunner, and H. U. Stäubli. 1998. Effect of cyclic preconditioning on the tensile properties of human quadriceps tendons and patellar ligaments. *Knee Surg. Sports Traumatol. Arthrosc.* 6 (*Suppl 1*):S56–S61.
18. Asundi, K. R., K. Kursa, …, D. M. Rempel. 2007. In vitro system for applying cyclic loads to connective tissues under displacement or force control. *Ann. Biomed. Eng.* 35:1188–1195.
19. Abramowitch, S. D., and S. L. Woo. 2004. An improved method to analyze the stress relaxation of ligaments following a finite ramp time based on the quasi-linear viscoelastic theory. *J. Biomech. Eng.* 126:92–97.
20. Provenzano, P., R. Lakes, …, R. Vanderby, Jr. 2001. Nonlinear ligament viscoelasticity. *Ann. Biomed. Eng.* 29:908–914.
21. Lam, T. C., C. B. Frank, and N. G. Shrive. 1993. Changes in the cyclic and static relaxations of the rabbit medial collateral ligament complex during maturation. *J. Biomech.* 26:9–17.
22. Woo, S. L., M. A. Gomez, and W. H. Akeson. 1981. The time and history-dependent viscoelastic properties of the canine medial collateral ligament. *J. Biomech. Eng.* 103:293–298.
23. Liao, J., L. Yang, …, M. S. Sacks. 2007. The relation between collagen fibril kinematics and mechanical properties in the mitral valve anterior leaflet. *J. Biomech. Eng.* 129:78–87.

24. Stella, J. A., J. Liao, and M. S. Sacks. 2007. Time-dependent biaxial mechanical behavior of the aortic heart valve leaflet. *J. Biomech.* 40:3169–3177.
25. Sasaki, N., Y. Nakayama, …, A. Enyo. 1993. Stress relaxation function of bone and bone collagen. *J. Biomech.* 26:1369–1376.
26. Egan, J. M. 1987. A constitutive model for the mechanical behaviour of soft connective tissues. *J. Biomech.* 20:681–692.
27. Huang, C. Y., V. C. Mow, and G. A. Ateshian. 2001. The role of flow-independent viscoelasticity in the biphasic tensile and compressive responses of articular cartilage. *J. Biomech. Eng.* 123:410–417.
28. Puxkandl, R., I. Zizak, …, P. Fratzl. 2002. Viscoelastic properties of collagen: synchrotron radiation investigations and structural model. *Philos. Trans. R. Soc. Lond. B Biol. Sci.* 357:191–197.
29. Fung, Y. C. 1967. Elasticity of soft tissues in simple elongation. *Am. J. Physiol.* 213:1532–1544.
30. Fung, Y. C., N. Perrone, and M. Anliker. 1972. Stress strain history relations of soft tissues in simple elongation. *In* Biomechanics: Its Foundations and Objectives.. Prentice-Hall, Englewood Cliffs, NJ. 181–207.
31. Johnson, G. A., G. A. Livesay, …, K. R. Rajagopal. 1996. A single integral finite strain viscoelastic model of ligaments and tendons. *J. Biomech. Eng.* 118:221–226.
32. Nekouzadeh, A., K. M. Pryse, …, G. M. Genin. 2007. A simplified approach to quasi-linear viscoelastic modeling. *J. Biomech.* 40:3070–3078.
33. Woo, S. L. 1982. Mechanical properties of tendons and ligaments. I. Quasi-static and nonlinear viscoelastic properties. *Biorheology.* 19:385–396.
34. Woo, S. L., G. A. Johnson, and B. A. Smith. 1993. Mathematical modeling of ligaments and tendons. *J. Biomech. Eng.* 115(4B): 468–473.
35. Kwan, M. K., T. H. Lin, and S. L. Woo. 1993. On the viscoelastic properties of the anteromedial bundle of the anterior cruciate ligament. *J. Biomech.* 26:447–452.
36. Heim, A. J., W. G. Matthews, and T. J. Koob. 2006. Determination of the elastic modulus of native collagen fibrils via radial indentation. *Appl. Phys. Lett.* 89:181902.
37. Wenger, M. P. E., L. Bozec, …, P. Mesquida. 2007. Mechanical properties of collagen fibrils. *Biophys. J.* 93:1255–1263.
38. Grant, C. A., D. J. Brockwell, …, N. H. Thomson. 2008. Effects of hydration on the mechanical response of individual collagen fibrils. *Appl. Phys. Lett.* 92:233902–233902-3.
39. Grant, C. A., D. J. Brockwell, …, N. H. Thomson. 2009. Tuning the elastic modulus of hydrated collagen fibrils. *Biophys. J.* 97:2985–2992.
40. Graham, J. S., A. N. Vomund, …, M. Grandbois. 2004. Structural changes in human type I collagen fibrils investigated by force spectroscopy. *Exp. Cell Res.* 299:335–342.
41. van der Rijt, J. A., K. O. van der Werf, …, J. Feijen. 2006. Micromechanical testing of individual collagen fibrils. *Macromol. Biosci.* 6:697–702.
42. Heim, A. J., T. J. Koob, and W. G. Matthews. 2007. Low strain nanomechanics of collagen fibrils. *Biomacromolecules.* 8:3298–3301.
43. Yang, L., K. O. van der Werf, …, J. Feijen. 2007. Micromechanical bending of single collagen fibrils using atomic force microscopy. *J. Biomed. Mater. Res. A.* 82:160–168.
44. Yang, L., K. O. van der Werf, …, J. Feijen. 2008. Mechanical properties of native and cross-linked type I collagen fibrils. *Biophys. J.* 94:2204–2211.
45. Eppell, S. J., B. N. Smith, …, R. Ballarini. 2006. Nano measurements with micro-devices: mechanical properties of hydrated collagen fibrils. *J. R. Soc. Interface.* 3:117–121.
46. Shen, Z. L., M. R. Dodge, …, S. J. Eppell. 2008. Stress-strain experiments on individual collagen fibrils. *Biophys. J.* 95:3956–3963.
47. Shen, Z. L., M. R. Dodge, …, S. J. Eppell. 2010. In vitro fracture testing of submicron diameter collagen fibril specimens. *Biophys. J.* 99:1986–1995.
48. Svensson, R. B., T. Hassenkam, …, S. Peter Magnusson. 2010. Viscoelastic behavior of discrete human collagen fibrils. *J. Mech. Behav. Biomed. Mater.* 3:112–115.
49. Shen, Z. L. 2010. Tensile mechanical properties of isolated collagen fibrils obtained by microelectromechanical systems technology. Ph.D. thesis. Case Western Reserve University, Cleveland, OH. 106–140.
50. Wittwer, J. W., M. S. Baker, and L. L. Howell. 2006. Robust design and model validation of nonlinear compliant micromechanisms. *J. Microelectromech. Syst.* 15:33–41.
51. Trotter, J. A., G. Lyons-Levy, …, T. J. Koob. 1995. Covalent composition of collagen fibrils from the dermis of the sea cucumber, *Cucumaria frondosa*, a tissue with mutable mechanical properties. *Comp. Biochem. Physiol. A.* 112:463–478.
52. Gautieri, A., S. Vesentini, …, M. J. Buehler. 2011. Hierarchical structure and nanomechanics of collagen microfibrils from the atomistic scale up. *Nano Lett.* 11:757–766.
53. Leikin, S., V. A. Parsegian, …, G. E. Walrafen. 1997. Raman spectral evidence for hydration forces between collagen triple helices. *Proc. Natl. Acad. Sci. USA.* 94:11312–11317.
54. Leikin, S., D. C. Rau, and V. A. Parsegian. 1994. Direct measurement of forces between self-assembled proteins: temperature-dependent exponential forces between collagen triple helices. *Proc. Natl. Acad. Sci. USA.* 91:276–280.
55. Buehler, M. J. 2006. Atomistic and continuum modeling of mechanical properties of collagen: elasticity, fracture, and self-assembly. *J. Mater. Res.* 21:1947–1961.
56. Gautieri, A., M. J. Buehler, and A. Redaelli. 2009. Deformation rate controls elasticity and unfolding pathway of single tropocollagen molecules. *J. Mech. Behav. Biomed. Mater.* 2:130–137.